J. Agr. Sci. Tech. (2015) Vol. 17: 287-298

Prediction of Paddy Moisture Content during Thin Layer Drying Using Machine Vision and Artificial Neural Networks

I. Golpour[1], R. Amiri Chayjan[1*], J. Amiri Parian[1], and J. Khazaei[2]

ABSTRACT

The goal of this study was to predict the moisture content of paddy using machine vision and artificial neural networks (ANNs). The grains were dried as thin layer with air temperatures of 30, 40, 50, 60, 70, and 80°C and air velocities of 0.54, 1.18, 1.56, 2.48 and 3.27 ms^{-1}. Kinetics of *L*a*b were measured. The air temperature, air velocity, and *L*a*b** values were used as ANN inputs. The results showed that with increase in drying time, L* decreased, but *a** and *b** increased. The effect of air temperature and air velocity on the *L*a*b** values were significant (P< 0.01) and not significant (P> 0.05), respectively. Changing of color values at 80°C was more than other temperatures. The optimized ANN topology was found as 5-7-1 with Logsig transfer function in hidden layer and Tansig in output layer. Mean square error, coefficient of determination, and mean absolute error of the optimized ANN were 0.001, 0.9630, and 0.031, respectively.**

Keywords: Back propagation neural network, Color features, Image processing, Rice.

INTRODUCTION

In Iran, rice (*Oryza sativa L.*) is considered as a strategic product, for its economical and nutritive values. It is cultivated in the north of the country extensively. To prevent rice damage following harvest of a high moisture content crop, paddy should be dried to such a level of moisture content that will supply safe storage by decreasing fissures. The allowable moisture content of paddy is 11-13% for safe storage, safe milling and subsequent safe storage as milled rice. If the moisture content of paddy is inappropriate for storage, it will be exposed to fungal diseases and chemical reactions and damaged after paddy husking (Mehdizadeh and Zomorodian, 2009).

Thin-layer drying is the process of removing water from a porous media by evaporation, in which drying air is passed through a thin layer of the material until equilibrium moisture content (EMC). Moisture removal from an agricultural product depends on drying air temperature, velocity, relative humidity, variety, and maturity. Hence, various isolated and combined methods are involved in moisture removal from a grain (Couto, 2002). Mathematical models of thin layer hot air drying have been studied in drying of fruits, vegetables, seafood, and some other agricultural products, such as mushroom and pollen (Midilli *et al.*, 1999), grape (Yaldiz *et al.*, 2001), eggplant (Ertekin and Yealdiz, 2004) and apple (Sacilik and Elicin, 2006).

In recent years, image analysis has been developed to evaluate food quality. Developed digital camera and related software proved to be an ideal combination for rapid, cheap, and accurate color measure

[1] Department of Biosystems Engineering, Faculty of Agriculture, Bu-Ali Sina University, Hamedan, Islamic Republic of Iran.
[*] Corresponding author; e-mail: amirireza@basu.ac.ir
[2] Department of Agricultural Technical Engineering, College of Abouraihan, University of Tehran, Islamic Republic of Iran.

[DOR: 20.1001.1.16807073.2015.17.2.20.3]

of various food products (Yam and Papadakis, 2004).

Determination of color can be carried out by visual inspection instruments. Determination of color by human inspection is extremely varied from observer to observer. Therefore, standard colors are often used, measured by *L*a*b** units, using either a colorimeter or specific data acquisition and image processing systems. The *L*a*b** is an international standard for color measurements, adopted by the Commission Internationale d'Eclairage (CIE) in 1976 and widely used in agriculture. *L** is the luminance or lightness component, which ranges from 0 to 100, *a** (from green to red) and *b** (from blue to yellow) are the two chromatic components, which range from –120 to 120 (Mohebbi *et al*., 2011; Wan *et al*., 2011; Afshari-Jouybari and Farahnaky, 2011). In the *L*a*b** space, the color perception is uniform, which means that the Euclidean distance between two colors corresponds approximately to the color difference perceived by the human eye (Hunt, 1991).

During drying process of fruits and vegetables, mathematical modeling could be a suitable approach to predict the quality indices of the products (Mohammed, 2011). For instance, Page model was successfully used to describe the drying characteristics of agricultural materials such as red chili and tomato slices (Gupta *et al*., 2002; Doymaz, 2007).

Drying of agricultural materials is a complex and non-linear process with long time delay. Therefore, it is very difficult to establish a precise mathematical model for grain drying control (Cao and Wang, 2002).

Artificial neural network (ANN) is a non-linear modeling that is generally used to model complex relationships between inputs and output parameters. A more realistic and accurate predictions can be obtained through ANN analysis (Akin and Akba, 2010). Artificial neural network was successfully used to describe the drying characteristics of agricultural crops such as jackfruit bulbs, leather, strawberries and grapes (Bala *et al*., 2005; Menli *et al*., 2009; Kassem *et al*., 2010) to model temperature in vacuum drying (Poonnoy *et al*., 2007a) and to estimate moisture ratio of mushroom undergoing microwave vacuum drying (Poonnoy *et al*., 2007b). Bakhshipour *et al*. (2012) used several ANN models to predict the moisture content of raisin during drying. Results indicated that machine vision and ANN were appropriate methods to predict moisture content of raisin with acceptable precision (R^2= 99.84%).

No study has been reported about prediction of paddy moisture content prediction by image processing and ANN method. Also, kinetics of paddy color change during thin layer drying is not available. The aim of this study was to model paddy moisture content during hot air thin layer drying process using color indices of paddy grains, image processing, and neural network approach.

MATERIALS AND METHODS

Sample Preparation

One popular paddy cultivar in Iran is Fajr. The samples were supplied from Rice Research Centers of Amol, Iran. The samples were stored in two layers of plastic and were placed in a refrigerator at 3±1°C. A laboratory oven was utilized to determine the initial moisture content of paddy samples. The oven was set at 130°C for 24 hours (ASAE, 2000). Measurements were replicated three times. The average moisture content of paddy samples was 21.21% (db). Bulk density of the samples was 751.65±16.4 kg m^{-3}.

Drying Process and Imaging System

Drying treatments were implemented in a laboratory thin layer dryer (Figure 1). The experiments were performed at six air temperatures (80, 70, 60, 50, 40, and 30°C)

[DOR: 20.1001.1.16807073.2015.17.2.20.3]

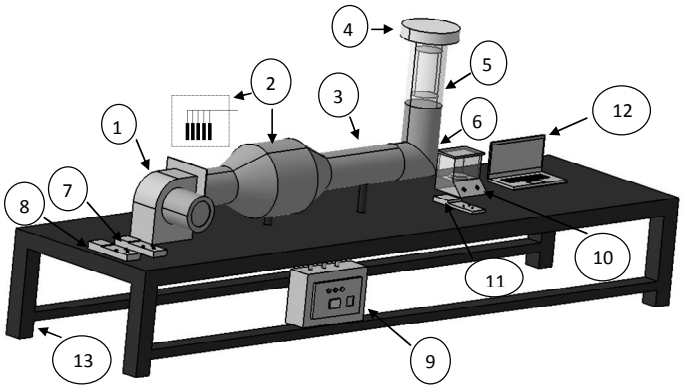

Figure 1. Schematic diagram of thin-layer dryer: (1) Fan and electrical motor; (2) Heating elements;(3) Duct and tunnel; (4) Chamber cap; (5) Drying chamber; (6) Mixing chamber; (7) Temperature and moisture meter; (8) Anemometer, (9) Thermostat and invertor; (10) Digital balance; (11) Input and output air temperature recorder; (12) Notebook, and (13) Chassis.

and five air velocities (0.54, 1.18, 1.56, 2.48, and 3.27 m s^{-1}) in three replications.

For each test, 30 g of paddy was dried as thin layer in the drying chamber. Moisture loss was intermittently measured by taking out the drying chamber and weighing on the digital balance with a precision of 0.01 g on time steps. Drying continued until a moisture content of 11-13% db. After each weighing, the sample images were also taken by a scanner (Hp scanjet G3110) with 300 dpi resolution (540×360 pixels). The sample was placed on the scanner surface covered with a silky fabric to take image. For each picture, the *L*a*b** values of the images were calculated and were used for paddy moisture prediction.

Image Preprocessing and Color Measurement

The body diagram of preprocessing approaches used in this study is shown in Figure 2. The entire algorithm for preprocessing of full images and color analysis were written in MATLAB R2010a. In this algorithm, transformation of RGB (red, green and blue) to *L*a*b** in two steps was performed using "makecform" and "applycform". In the first step, the transformation of RGB to XYZ was conducted and in the next step, transformation of XYZ was performed to *L*a*b** (Hunt, 1991). Parameter *L** refers to the lightness of the samples, ranging between black (L= 0) and white (L= 100). Parameter *a** is a chromatic component ranging between green and magenta (negative values indicate green while positive values indicate magenta). Parameter *b** changes from blue to yellow (negative values indicate blue while positive values indicate yellow). Values of *a** and *b** range from -120 to +120.

Artificial Neural Networks (ANN) Modeling

A multiple layer back propagation neural network model was applied to obtain a non-linear relationship between input variables

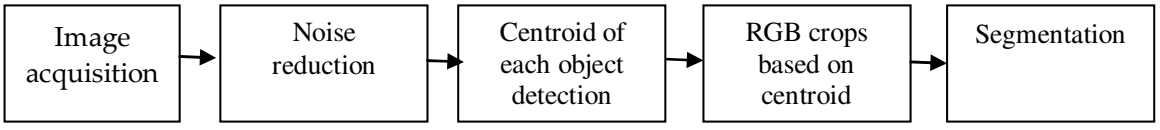

Figure 2. Image preprocessing algorithm.

[DOR: 20.1001.1.16807073.2015.17.2.20.3]

(air temperature, air velocity, L*, a* and b*) and output variable (final moisture content) as shown in Figure 3. This network is feed forward back propagation (FFBP). Input data were divided into two parts: 70% of the data for training and the remaining 30% of the data for testing, which were randomly selected. The input and output data were normalized between [0, 1] and [-1, 1]. Neural network toolbox of Matlab 7 was used to model the data.

Several topologies were tested by changing the number of neurons in hidden layer. The artificial neural network (ANN) was trained with Levenberg-Marquardt (LM) learning algorithm which is known to be very efficient (Bakhshipour *et al*., 2012). The network in this study stopped when target error decreased to less than 0.01.

To find a suitable topology, mean square error was used to minimize the error function (Momenzadeh *et al*., 2012):

$$MSE = \frac{1}{MN}\sum_{P=1}^{M}\sum_{i=1}^{N}(S_{ip} - T_{ip})^2 \quad (1)$$

Where, *MSE* is mean squares error, S_{ip} is output ANN for neuron *i* and pattern *p* and T_{ip} is the output of goal in neuron *i* and pattern *p* (moisture content), *N* is the number of output layer neuron and *M* is the number of test patterns. Moreover, the coefficient of determination (R^2) and mean absolute error (MAE) were also used to predict the ANN performance:

$$R^2 = \left(1 - \frac{\sum_{k=1}^{M}[S_k - T_k]}{\sum_{k=1}^{M}[S_k - T_m]}\right)\left\{T_{m=}\frac{\sum_{k=1}^{n}S_k}{n}\right\} \quad (2)$$

$$MAE = \frac{1}{n}\sum_{k=1}^{n}|S_k - T_k| \quad (3)$$

Where, *n* is the number of training pattern and *MAE* is the mean absolute error.

Statistical Analysis

Experimental data for the different parameters were implemented with factorial statistical design in complete randomized design by using SAS (ver. 9.1) software, and the mean values were compared through LSD at 0.05 and 0.01 levels and ANOVA table is presented.

RESULTS AND DISCUSSION

Drying Curves

Paddy moisture content variations with drying time are illustrated at different air velocities (0.51, 1.18, 1.56, 2.48 and 3.27 m s^{-1}) and air temperatures (30, 40, 50, 60, 70 and 80°C) in Figure 4. According to the

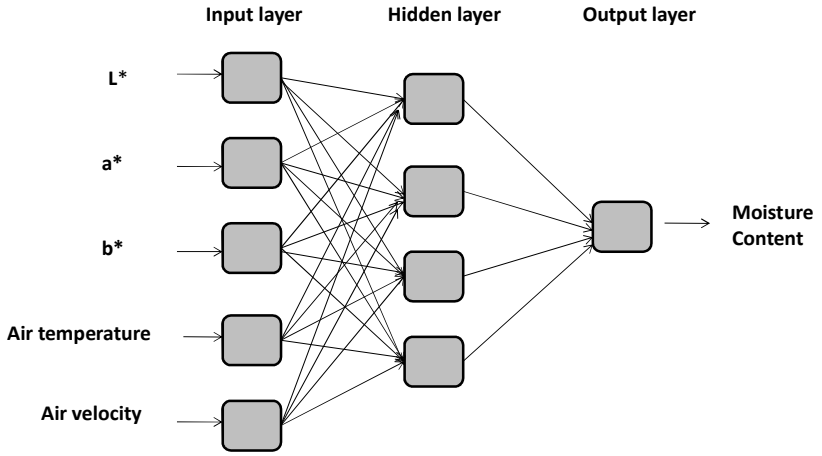

Figure 3. The ANN structure for prediction of paddy moisture content. L*: lightness, a*: chromatic component ranging between green and magenta, b*: changes from blue to yellow.

[DOR: 20.1001.1.16807073.2015.17.2.20.3]

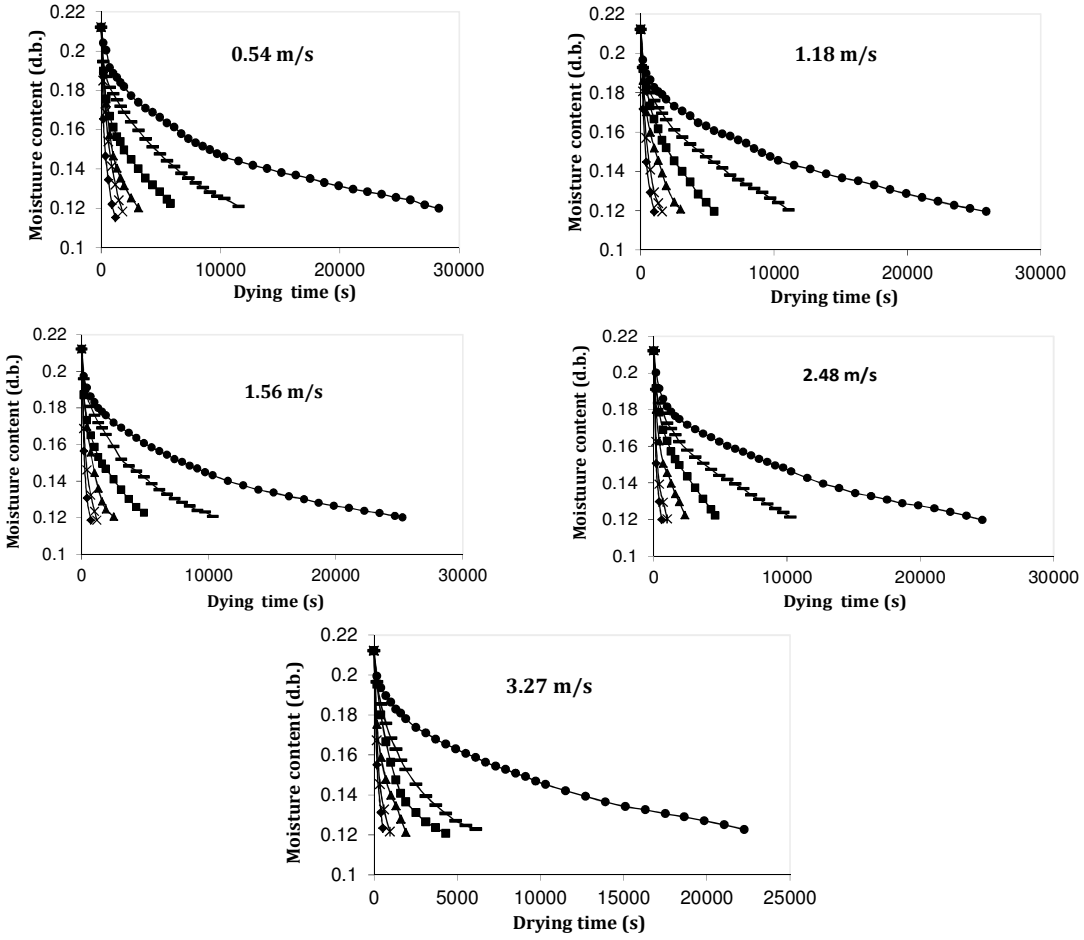

Figure 4. Drying curves of paddy at different air temperatures [(●) 30°C , -40°C; (▪) 50°C; (▲) 60°C; (×) 70°C, and (♦) 80°C] and air velocities.

results, drying air temperature played an important role in drying process. When the air temperature was increased, the drying time was reduced. At the initial period of drying process, moisture content decreased significantly in the experiments. Also, as can be seen in Figure 4 for air velocity of 1.18 m s^{-1}, the drying time of paddy were 25,920, 11,100, 5,520, 3,000, 1,620 and 1,020 seconds at air temperature of 30, 40, 50, 60, 70, and 80°C, respectively. The lowest drying time was acquired at air temperature of 80°C. Similar results were reported by Ratti *et al*. (2007) for garlic, Arabhosseini *et al.* (2009) for tarragon, Arumuganathan *et al.* (2009) for mushroom, and Kaleta and Górnicki (2010) for red beet drying.

In general, with increasing air temperature, final drying time of paddy was decreased, because at the higher air temperature and air velocity, temperature difference between the drying air and paddy raises the surface heat transfer coefficient, which affects the heat and mass transfer rate. Some researchers reported similar results in drying of fruits and vegetables such as apples and garlic (Sacilik and Elicin, 2006; Ratti *et al*., 2007).

Color Analysis

The average measured color indices of the fresh paddy were 60.6, -7.31 and 14.72 for *L*, a** and *b**, respectively. Color change

[DOR: 20.1001.1.16807073.2015.17.2.20.3]

conditions and the effects of the various air temperatures, different air velocities, and *L*a*b** values showed that the color changing characteristics at higher air temperature were more than on other air temperatures. As a result, the changing of color values at 80°C was more than other temperatures (Figures 5-7) because, with increasing air temperature, the husk surface of paddy became darker and the variations of the sample color increased after drying process. The average values of *L*, a** and *b** were obtained in the drying process at three iterations. The *L** values of paddy during the drying process decreased with increase in drying time (Figure 5). Brightness change of the dried samples can be taken as a measurement of browning (Lee and Coates, 1999). This result is similar to that of Wan *et al.* (2011). Values of *a** and *b** increased with increase in drying time (Figures 6 and 7), so that these results were similar to those reported by Shafafi Zenozian *et al.* (2008). Paddy sample was darker compared to the original sample after drying (with the final moisture content about 11-13% db). Color change indices at various air temperatures are presented in Figures 5-7. At all air velocities, the lowest *L*a*b** values corresponded to air temperature of 30°C and the highest values were recorded at air temperature of 80°C. This non-linearity in color feature changes may be due the distortion resistance of the paddy crust at the early period of moisture decline. In other words, at the initial stages of drying, free water was removed from capillary tubes without causing a significant variation in the color of the paddy. After this stage, the color features gradually changed. One of the other reasons of the paddy color changes was pigment degradation of paddy.

Statistical Analysis

Data acquired from laboratory experiments and machine vision system (MVS) were analyzed statistically. Analysis of variance (ANOVA) revealed that air temperature of drying had highly significant effect on *L*, a** and *b** values as well as on drying time at probability level of 0.01 (Table 1). Similar results have been reported by Mohebbi *et al.* (2009) for shrimp. The air velocity had no significant effect on drying time because the air velocity range at high air temperature was low and limited. Similar results have been reported for wheat (Sun and Woods, 1994) and rapeseed (Patak, 1991). Also, interaction of air velocity with air temperature had no significant effect on the *L*, a** and *b** values.

Table 2 shows the mean values for drying time and color features at various air temperatures. The highest value of *L** was observed at 30°C (Figure 5). Temperature had significant effect on drying time, thus, six different levels were obtained in the drying process at six different drying temperatures (Table 2). These six different temperature levels created two, three, and five different significant levels for *L*, a** and *b**, respectively. *L** was not significant at air temperatures of 70 and 80°C (Table 2). The highest value of *a** was recorded for the dried samples at 80°C (Figure 6), while there was no significant difference between 70°C and 80°C ($P > 0.05$) (Table 2). The highest *b** value was observed at 80°C (Figure 7) which had a significant difference with 70°C ($P < 0.05$). The color changes may be due to either the non-enzymatic or enzymatic reactions during the drying process (Aguilera, 2003). When food processing is heat-processed, a number of chemical reactions occur. One of them is the Millard reaction, known to be responsible for non-enzymatic browning. The Millard reaction involves the reaction of an aldehyde and an amine (usually a protein or amino acid) and is highly temperature-dependent. Bingol *et al*. (2012) also reported that the *L** value decreased while *a** value increased during grape drying process under the grape's different pretreatment conditions.

[DOR: 20.1001.1.16807073.2015.17.2.20.3]

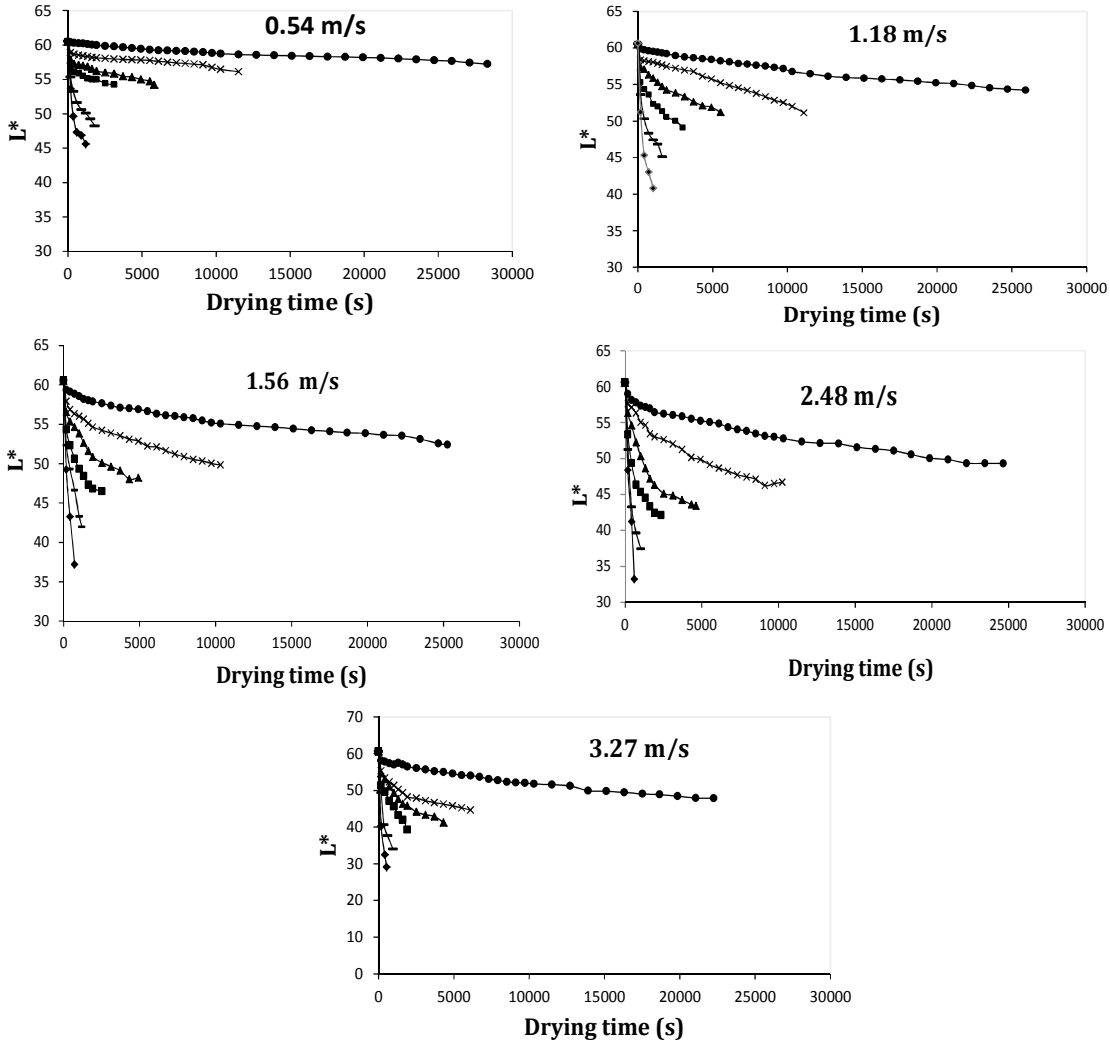

Figure 5. Variation of L* (lightness) of paddy samples during drying at different air velocities (0.54; 1.18; 1.56; 2.48, and 3.27 m s^{-1}) and air temperatures [(●) 30°C , -40°C; (▪) 50°C; (▲) 60°C; (×) 70°C, and (♦) 80°C].

Table 1. Analysis of variance of the effect of air velocity (V) and air temperature (T) on color features and drying time of paddy.

Source	DOF	L* [a]	a* [b]	b* [c]	Drying time (s)
V [d]	4	41.42^{ns}	0.40^{ns}	1.30^{ns}	1398479^{ns}
T [e]	5	348.89^{**}	17.71^{**}	553.91^{**}	1567240^{**}
V×T	20	2.36^{ns}	0.45^{ns}	1.30^{ns}	1311869^{ns}
Error	60	17.26	0.16	0.85	763556
CV (%)		8.27	9.94	3.7	10.26

[a] Lightness, [b] Chromatic component ranging between green and magenta, [c] Changes from blue to yellow, [d] Air velocity (m s^{-1}); [e] Air temperature (°C), ns: Non-significant., ** Significant at 1% level.

[DOR: 20.1001.1.16807073.2015.17.2.20.3]

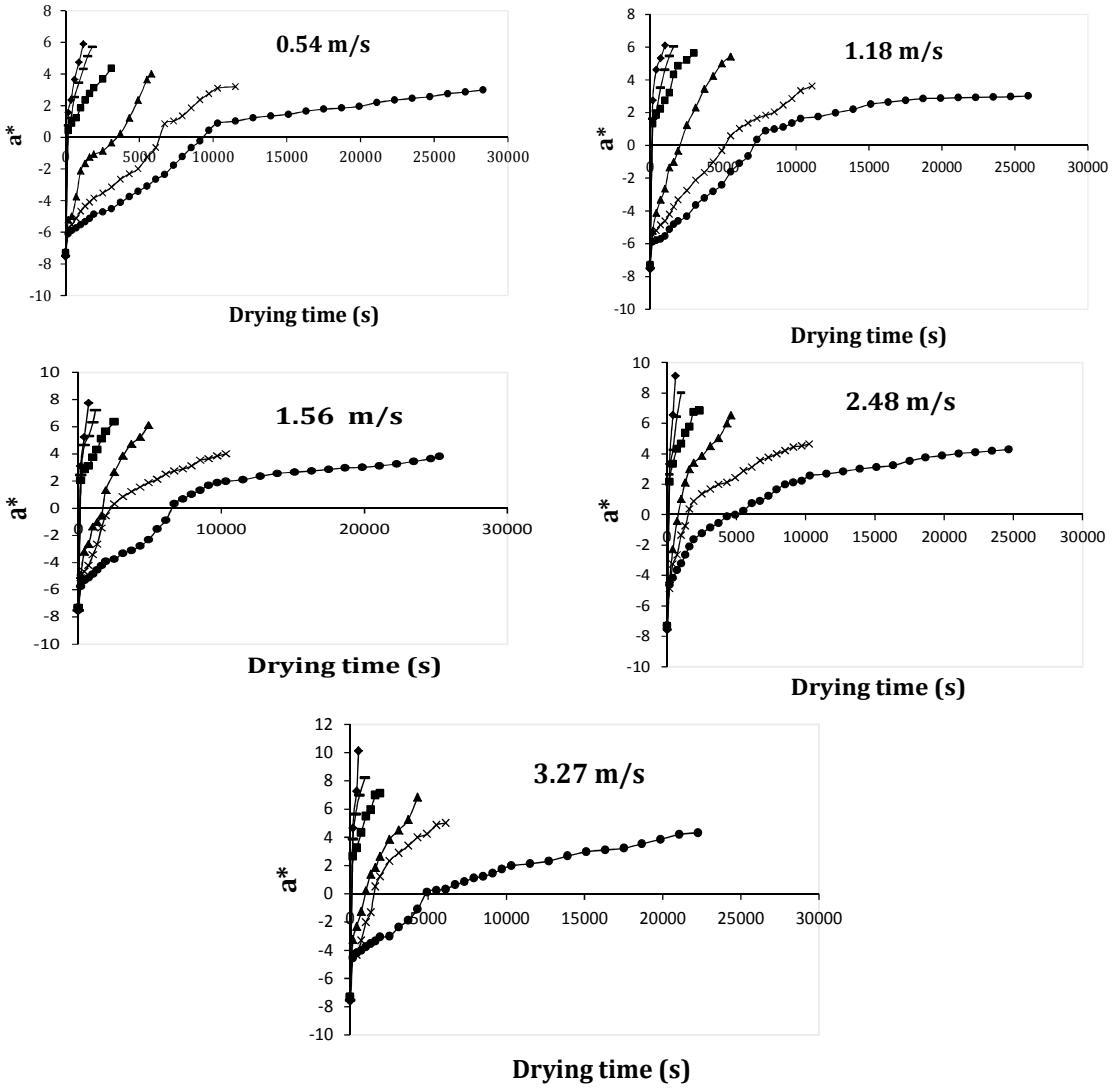

Figure 6. Variation of a* (chromatic component ranging between green and magenta) of paddy samples during drying at different air velocities (0.54; 1.18; 1.56; 2.48, and 3.27 m s^{-1}) and air temperatures [(●) 30°C, -40°C; (▪) 50°C; (▲) 60°C; (×) 70°C, and (♦) 80°C].

Table 2. The mean comparison effects of temperature treatment on the color features and moisture content.

T (°C)	Drying time (s)	L* [a]	a* [b]	b* [c]
30	27983[a d]	54.86[g]	2.71[j]	19.48[n]
40	11217[b]	53.96[gh]	2.99[j]	19.85[n]
50	5837[c]	52.02[gh]	3.80[k]	20.77[o]
60	3152[d]	51.56[h]	4.28[l]	24.77[p]
70	1816[e]	45.73[i]	5.24[m]	30.58[q]
80	1078[f]	42.78[i]	5.25[m]	33.87[r]

[a] Lightness, [b] Chromatic component ranging between green and magenta, [c] Changes from blue to yellow, [d] Different letters means different clusters.

[DOR: 20.1001.1.16807073.2015.17.2.20.3]

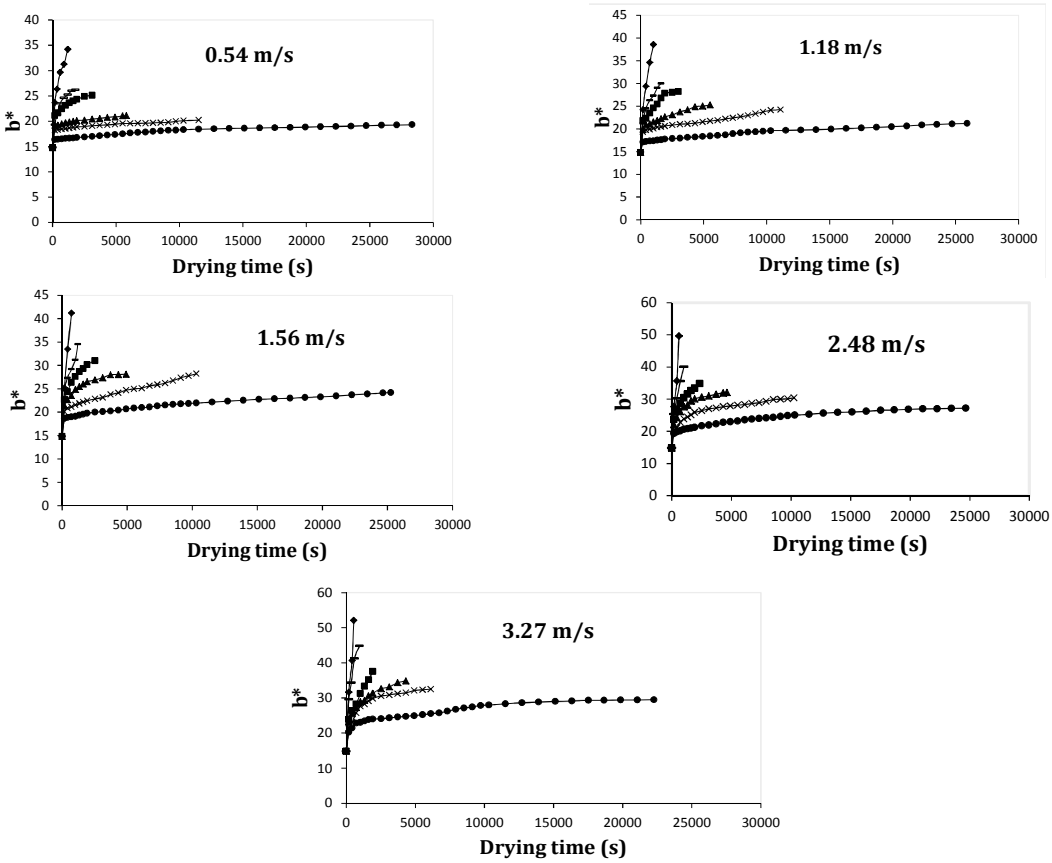

Figure 7. Variation of b* (Changes from blue to yellow) of paddy samples during drying at different air velocities (0.54; 1.18; 1.56; 2.48, and 3.27 m s^{-1}) and air temperatures (●30, - 40, ▪50, ▲60, ×70, and ♦80 °C).

Moisture Content Prediction by ANN

The artificial neural network with one hidden layer was utilized to learn and predict the correlation between input and output data. In this network, input data were air temperature, air velocity, *L*, a*,* and *b** and output data was moisture content. To determine the optimum number of neurons in hidden layer, training was utilized for 5-*x*-1 structure, in which the number of input parameters was five and the number of output parameters was one. The number of neurons in the hidden layer *x* was changed from 1 to 10. After training and testing the network, the results indicated that the best training performance to model moisture content was obtained with topology 5-7-1 and transfer functions of Logsig and Tansig in hidden layer and output layers (Table 3). This optimized structure had the lowest mean square error (MSE= 0.00105) during training process. Figure 8 illustrates the relationship and coefficient of determination between the experimental and predicted moisture content of paddy after testing process using artificial neural network. Figure 8 proved that the experimental against predicted values of testing points were consistently scattered around the $y= x$ regression line. The optimized network presented the best result with the maximum value of coefficient of determination (R^2= 0.9630) and the lowest value of mean absolute error (MAE= 0.031) (Table 3). Chayjan *et al*. (2007) predicted the layer moisture content of paddy with neural network of feed forward back propagation, with topology of 3-5-4-1and R^2= 0.9949.

[DOR: 20.1001.1.16807073.2015.17.2.20.3]

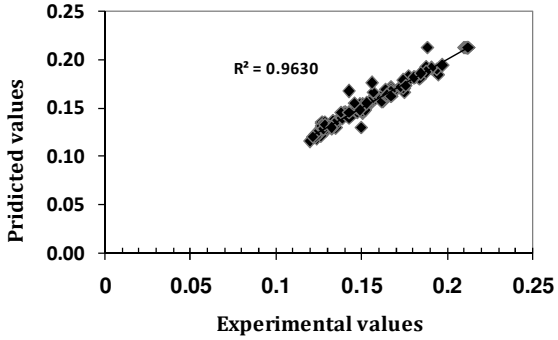

Figure 8. The scatter plot of experimental values vs. predicted values of moisture content using the optimized ANN for testing data set.

Table 3. Best selected topologies including treshold functions, topologies, for feed forward back propagation network.

Threshold function	Topology	Epoch	MSE	R^2	MAE
Logsig-Tansig	5-7-1	18	0.00105	0.9630	0.031
Logsig-Purelin	5-5-1	19	0.00371	0.9567	0.035
Tansig-Purelin	5-6-1	83	0.00530	0.9557	0.035
Tansig-Tansig	5-6-1	14	0.00078	0.9551	0.078
Purelin- Purelin	5-3-1	13	0.00350	0.9337	0.038
Purelin-Ttansig	5-10-1	2	0.00248	0.8710	0.059
Tansig-Logsig	5-8-1	18	0.00204	0.7260	0.077
Purelin-Logsig	5-11-1	4	0.00093	0.7201	0.063
Logsig-Logsig	5-8-1	10	0.00971	0.6586	0.084

CONCLUSIONS

The drying behavior of paddy in a thin layer dryer and relationship of moisture content of the samples with color features at six air temperatures of 30, 40, 50, 60, 70, and 80°C and five air velocities of 0.54, 1.18, 1.56, 2.48, and 3.27 m s^{-1} using machine vision system was investigated. The air temperature had significant effect on the *L*, a*,* and *b** values at probability of 0.01 (P< 0.01). The *L** values decreased in the drying process and the *b** (yellowness) and *a** (redness) values increased with increasing the drying time. Changing of color values at 80°C was more than the other temperatures. Artificial neural networks (ANNs) was a proper method for predicting moisture content of paddy using extracted color features with image analysis. Best training performance to model moisture content was obtained with topology of 5-7-1 and transfer functions of Logsig and Tansig in hidden layer and output layers (Table 3). Results showed that the optimized network presented *R2*= 0.9630 for prediction of moisture content of paddy using image processing technique and drying characteristics.

ACKNOWLEDGEMENT

The authors appreciatively acknowledge the Amol Rice Research Institute for providing paddy samples and we thank Dr. Zamani and Mr Seyedi of Bu Ali Sina University for help in statistical analysis of this research.

REFERENCES

1. Afshari-Jouybari, H. and Farahnaky, A. 2011. Evaluation of Photoshop Software Potential for Food Colorimetry. *J. Food Eng.*, **106:** 170-175.
2. Akin, D. and Akba, B. 2010. A Neural Network (NN) Model to Predict Intersection Crashes Based upon Driver, Vehicle and

[DOR: 20.1001.1.16807073.2015.17.2.20.3]

Roadway Surface Characteristics. *Sci. Res. Essays,* **5(19)**: 2837-2847.
3. Aguilera, J. M. 2003. Drying and Dried Products under the Microscope. *Int. J. Food Sci. Tech.,* **9(3):**137–143.
4. Arabhosseini, A., Huisman, W., Van Boxtel, A. and Muller, J. 2009. Modeling of Thin Layer Drying of Tarragon (*Artemisia dracunculus* L.). *Indust. Crops Prod.,* **29**: 53–59.
5. Arumuganathan, T., Manikantan, M.R., Rai, R. D., Anandakumar, S. and Khare, V. 2009. Mathematical Modeling of Drying Kinetics of Milky Mushroom in a Fluidized Bed Dryer. *Int. Agrophysics*, **23:** 1-7.
6. ASAE. 2000. ASAE Standard S352.2. Moisture Measurement: Unground Grain and Seeds. 47th Edition. ST. Joseph, MI, USA.
7. Bakhshipour, A., Jafari, A. and Zomorodian, A. 2012. Vision Based Features in Moisture Content Measurement during Raisin Production. *World Appl. Sci. J.*, **17 (17):** 860-869.
8. Bala, B. K., Ashraf. M. A., Uddin, M. A. and Janjai, S. 2005. Experimental and Neural Network Prediction of the Performance of a Solar Tunnel Drier for Drying Jackfruit Bulbs and Leather. *J. Food Process Eng.*, **28:** 552-566.
9. Bingol, G., Roberts, J. S., Murat, O., Balaban, M. and Devres, Y. O. 2012. Effect of Dipping Temperature and Dipping Time on Drying Rate and Color Change of Grapes. *Drying Technol.,* **30:** 597-606.
10. Cao, C. and Wang, X. B. 2002. Automatic Control of Grain Driers. *Modernizing Agric.*, **2:** 40–44.
11. Chayjan, R. A., Khoshtaghaza, M. H., Montazer, G. A. and Minaei, S. 2007. Estimation of Paddy Layers Moisture Content Using Artificial Neural Networks. *Iran. J. Agric. Sci.,* **38(1):** 113-123.
12. Couto, S. M. 2002. Modeling Grain Drying as Discharge of an RC Electrical Circuit. *Trans. ASAE*, **45:** 1445–54.
13. Doymaz, I. 2007. Air-drying Characteristics of Tomatoes. *J. Food Eng.*, **78:** 1291-1297.
14. Ertekin, C. and Yaldiz, O. 2004. Drying of Eggplant and Selection of a Suitable Thin Layer Drying Model. *J. Food Eng.,* **63:** 349-359.
15. Gupta, T., Ahmed, J., Shivhare, U. S. and Raghavan, G. S. V. 2002. Drying Characteristics of Red Chili. *Drying Technol.*, **20:** 1975–1987.
16. Hunt, R.W.G. 1991. Measuring Color. 2nd Edition, Ellis Horwood, New York, PP. 313.
17. Kaleta, A. and Górnicki, K. 2010. Some Remarks on Evaluation of Drying Models of Red Beet Particles. *Energy Conv. Manage.,* **51**: 2967–2978.
18. Kassem, A. S., Shokr, A. Z., Aboukarima, A. M. and Hamed, I. Y. 2010. Estimation of Moisture Ratio of Thompson Seedless Grapes Undergoing Microwave Drying Using Artificial Neural Network and Regression Models. J. Saudi Soc. *Agric. Sci.*, **9(1):** 23–47.
19. Kim, H. K., Jo, K. M., Kwon, D. Y. and Park, M. H. 1992. Effects of Drying tTemperature and Sulfiting on the Qualities of Dried Garlic Slices. *J. Korean Agric. Chem. Soc.,* **35(1):** 6–9.
20. Lee, H. S. and Coates, G. A. 1999. Thermal Pasteurization Effects on Colour of Red Grape Fruit Juices. *J. Food Sci.*, **64**: 663–666.
21. Madamba, P. S., Driscoll, R. H. and Buckle, K. A. 1996. The Thin-layer Drying Characteristics of Garlic Slices. *J. Food Eng.*, **29(1):** 75–97.
22. Mehdizadeh, Z. and Zomorodian, A. 2009. A Study of the Effect of Solar Drying System on Rice Quality. *J. Agr. Sci. Tech.,* **11**: 527-534.
23. Menli, T., Kirmaci, V. and Usta, H. 2009. Modeling of Freeze Drying Behaviors of Strawberries by Using Artificial Neural Network. *J. Thermal Sci. Technol.*, **29(2):** 11-21.
24. Midilli, A., Olgun, H. and Ayhan, T. 1999. Experimental Studies on Mushroom and Pollen Drying. *Int. J. Energy Res.*, **23(13):** 1143–1152.
25. Mohammed, A. A. 2011. Prediction of Quality Indices during Drying of Okra Pods in a Domestic Microwave Oven Using Artificial Neural Network Model. *African J. Agric. Res.*, **6(12):** 2680–2691.
26. Mohebbi, M., Akbarzadeh, M.R., Shahidi, F., Moussavi, M. and Ghoddusi, H. B. 2009. Computer Vision Systems (CVS) for Moisture Content Estimation in Dehydrated Shrimp. *Comput. Elect. Agric.*, **69:** 128–134.
27. Mohebbi, M., Shahidi, F., FathI, M., Ehtiati, A. and Noshad, M. 2011. Prediction of Moisture Content in Pre-osmosed and Ultrasounded Dried Banana Using Genetic Algorithm and Neural Network. *Food Bioprod. Proces.*, **84(4):** 362-366.
28. Momenzadeh, L., Zomorodian, A. and Mowla, A. 2012. Applying Artificial Neural Network for Drying Time Prediction of Green Pea in a

[DOR: 20.1001.1.16807073.2015.17.2.20.3]

Microwave Assisted Fluidized Bed Dryer. *J. Agric. Sci. Technol.*,**14:** 513–522.
29. Patak, P. T. 1991. Thin layer Drying Model for Rapeseed. *Trans. ASAE*, **34:** 2505–2508.
30. Poonnoy, P., Tansakul, A. and Chinnan, M. S. 2007a. Artificial Neural Network Modeling for Temperature and Moisture Content Prediction in Tomato Slices Undergoing Microwave-vacuum Drying. *J. Food Sci.,* **72(1):** 41– 47.
31. Poonnoy, P., Tansakul, A. and Chinnan, M. S. 2007b. Estimation of Moisture Ratio of a Mushroom Undergoing Microwave-vacuum Drying Using Artificial Neural Network and Regression Models. *Chem. Prod. Process Model.*, **2(3):** 1-13.
32. Ratti, C., Araya-Farias, M., Mendez-Lagunas, L. and Makhlouf, J. 2007. Drying of Garlic (*Allium sativum*) and Its Effect on Allicin Reterntion. *Drying Technol.*, **25(2):** 349–356.
33. Sacilik, K. and Elicin, A. K. 2006. The Thin Layer Drying Characteristics of Organic Apple Slices. *J. Food Eng.*, **73:** 281–289.
34. Shafafi Zenozian, M., Feng, H., Razavi, S. M. A., Shahidi, F. and Pourreza, H. R. 2008. Image Analysis and Dynamic Modeling of Thin-layer Drying of Osmotically Dehydrated Pumpkin. *J. Food Process. Preserv.*, **32:** 88–102.
35. Sun, D. W. and Woods, J. L. 1994. Low Temperature Moisture Transfer Characteristics of Wheat in Thin Layers. *Trans. ASAE.*, **37:** 1919–28.
36. Wan, P., Long, C. and Huang, X. 2011. A Detection Method of Rice Process Quality Based on the Color and BP Neural Network. *Conference of the 4th Computer and Computing Technologies in Agriculture*, 22-25 October, Nanchang, China, **344:** 25–34.
37. Yaldiz, O., Ertekin, C. and Uzun, H. I. 2001. Mathematical Modeling of Thin Layer Solar Drying of Sultan Grapes. *Energy*, **26:** 457–465.
38. Yam, K. L. and Papadakis, S. E. 2004. A Simple Digital Imaging Method for Measuring and Analyzing Color of Food Surfaces, *J. Food Eng.*, **61:** 137–142.

پیش بینی رطوبت شلتوک در طول خشک کردن لایه نازک با استفاده از ماشین بینایی و شبکه های عصبی مصنوعی

ا. گل پور، ر. امیری چایجان، ج. امیری پریان، ج. خزایی

چکیده

هدف از این مطالعه، پیش بینی رطوبت شلتوک با استفاده از ماشین بینایی و شبکه های عصبی مصنوعی (ANN*s*) است. دانه ها به صورت لایه نازک با درجه حرارت هوای ۳۰، ۴۰، ۵۰، ۶۰، ۷۰ و ۸۰ درجه سلسیوس و با سرعت هوای ۰/۵۴، ۱/۱۸، ۱/۵۶، ۲/۴۸ و ۳/۲۷ متر بر ثانیه خشک شدند. سینتیک L*a*b* ارزیابی شد. دمای هوا، سرعت هوا و مقادیر L*a*b* به عنوان ورودی ANN مورد استفاده قرار گرفت. نتایج نشان داد که با افزایش زمان خشک شدن، L* کاهش اما a* و b* افزایش یافت. تغییرات شاخص های رنگ در دمای ۸۰ درجه سیلسیوس بیشتر از سایر دماها بود. اثر دمای هوا بر روی مقادیر L*a*b* معنی دار ($p<0/01$) و اثر سرعت هوا معنی دار نبود ($P>0/05$). توپولوژی بهینه‌ی ANN به عنوان ۱-۷-۵ با تابع انتقال Logsig در لایه پنهان و Tansig در لایه خروجی یافت شد. میانگین مربع خطا، ضریب تعیین و میانگین خطای مطلق از ANN بهینه، به ترتیب ۰/۰۰۱، ۰/۹۶۳۰ و ۰/۰۳۱ بودند.

[DOR: 20.1001.1.16807073.2015.17.2.20.3]